# Off-axis electron orbits in realistic helical wigglers for free-electron-laser applications

J. Fajans, D. A. Kirkpatrick, and G. Bekefi
*Department of Physics and Research Laboratory of Electronics, Massachusetts Institute of Technology, Cambridge, Massachusetts 02139*
(Received 5 August 1985)

Off-axis electron orbits in free-electron-laser beams of finite thickness, subjected to combined helical wiggler and axial guide fields, have been studied analytically. A semiempirical equation for the electron velocity components, averaged over the electron's oscillatory (betatron) motion, has been derived as a function of the radial displacement of the electron guiding center. The predictions from the equation are compared with single-particle numerical simulations, and with free-electron-laser experiments. Good agreement is found.

## INTRODUCTION

Accurate prediction of the gain and output frequency of a free-electron laser (FEL) requires precise knowledge of the axial and transverse electron velocity. The full three-dimensional field of a helical wiggler magnet, $\mathbf{B}_w$, has a strong radial dependence. Moreover, many high-current experiments also use an axial guide magnetic field $\mathbf{B}_a$ superimposed on the wiggler field $\mathbf{B}_w$, thereby causing a resonance in the electron orbits. Consequently, except for a class of highly constrained electron orbits, it is generally difficult to predict the exact electron motion. This is particularly true in the neighborhood of the above-mentioned resonance $\Omega_a \approx k_w \beta_{||} c$, where $\Omega_a = eB_a/\gamma m_0 c$ is the relativistic cyclotron frequency in the axial guide magnetic field, $\gamma = (1-\beta_{||}^2-\beta_\perp^2)^{-1/2}$ is the relativistic energy factor, $\beta_{||} = v_{||}/c$ with $v_{||}$ the axial electron velocity and $\beta_\perp = v_\perp/c$ with $v_\perp$ the transverse electron velocity induced by the wiggler magnetic field, and $k_w = 2\pi/l$ is the wiggler wave number with $l$ the wiggler period.

In the original one-dimensional orbit theory,[1] the radial variations of the wiggler-field amplitude are neglected and the total externally applied axial plus wiggler field is assumed to be of the form

$$\mathbf{B} = \hat{\mathbf{e}}_z B_a + B_w[\hat{\mathbf{e}}_x \cos(k_w z) + \hat{\mathbf{e}}_y \sin(k_w z)] , \tag{1}$$

where $\hat{\mathbf{e}}_x$, $\hat{\mathbf{e}}_y$, and $\hat{\mathbf{e}}_z$ are unit vectors along the $x$, $y$, and $z$ axes, and $B_a$ and $B_w$ are the amplitudes of the guide and wiggler fields, respectively. This field configuration has the special virtue of possessing an easily derived class of highly desirable, purely helical electron orbits characterized by the fact that the axial and perpendicular electron velocities are constants of the motion.[1] These trajectories are specified by the simultaneous solution of the energy-conservation equation

$$1/\gamma^2 = 1-\beta_{||}^2-\beta_\perp^2 = \text{const} , \tag{2}$$

and the velocity relation

$$\beta_\perp = \frac{\Omega_w \beta_{||}}{k_w \beta_{||} c - \Omega_a} \quad (k_w \beta_{||} c \neq \Omega_a) , \tag{3}$$

where $\Omega_w = eB_w/\gamma m_0 c$ is the relativistic cyclotron frequency associated with the wiggler magnetic field. We note that in order to achieve the helical orbits given by Eqs. (2) and (3), the electrons must be launched into a wiggler field that has a slow, smooth introduction,[1,2] and the exact resonance $k_w \beta_{||} c = \Omega_a$ must be avoided.

In the case of a physically realizable wiggler field[3] that satisfies Maxwell's equations $\nabla \cdot \mathbf{B}_w = 0$ and $\nabla \times \mathbf{B}_w = \mathbf{0}$, the wiggler field $\mathbf{B}_w$ necessarily has a radial dependence. The combined axial and wiggler fields, expressed in cylindrical coordinates $(r, \phi, z)$, are given by

$$\mathbf{B} = \hat{\mathbf{e}}_z B_a + 2B_w \left[ \hat{\mathbf{e}}_r I_1'(k_w r)\cos(\phi - k_w z) - \hat{\mathbf{e}}_\phi \frac{I_1(k_w r)}{k_w r}\sin(\phi - k_w z) + \hat{\mathbf{e}}_z I_1(k_w r)\sin(\phi - k_w z) \right] , \tag{4}$$

where $I_1$ is the modified Bessel function. It has been shown[4] that if all the beam electrons enter the wiggler *exactly* on axis, and are then allowed to spiral out in the gradually increasing wiggler field, the electrons once again execute purely helical orbits, just as in the one-dimensional calculations described above. Now, however, the transverse electron velocity acquired in the magnetic field is given by the simultaneous solution of Eq. (2) and

$$\beta_\perp = \frac{2\Omega_w \beta_{||} I_1(\lambda)/\lambda}{k_w \beta_{||} c - \Omega_a - 2\Omega_w I_1(\lambda)} . \tag{5}$$

Here $\lambda = \beta_\perp/\beta_{||} = \pm k_w r$ is the normalized size of the orbit, such that $\lambda = -k_w r$ when $\Omega_a > k_w \beta_{||} c$, and $\lambda = +k_w r$ when $\Omega_a < k_w \beta_{||} c$.

In practical systems comprised of an electron beam of finite thickness, a large fraction of the electrons entering the wiggler are not axis centered, their orbits are not purely helical, and the axial and transverse electron velocities oscillate about mean values denoted by $\langle \beta_{||} \rangle$ and $\langle \beta_\perp \rangle$. This is illustrated in Fig. 1, which shows the trajectory of an electron propagating through a wiggler entrance and well into the constant-wiggler-amplitude region. In the entrance region, the wiggler converts a fraction of the axial velocity $\beta_{||} = v_{||}/c$ into perpendicular velocity

 

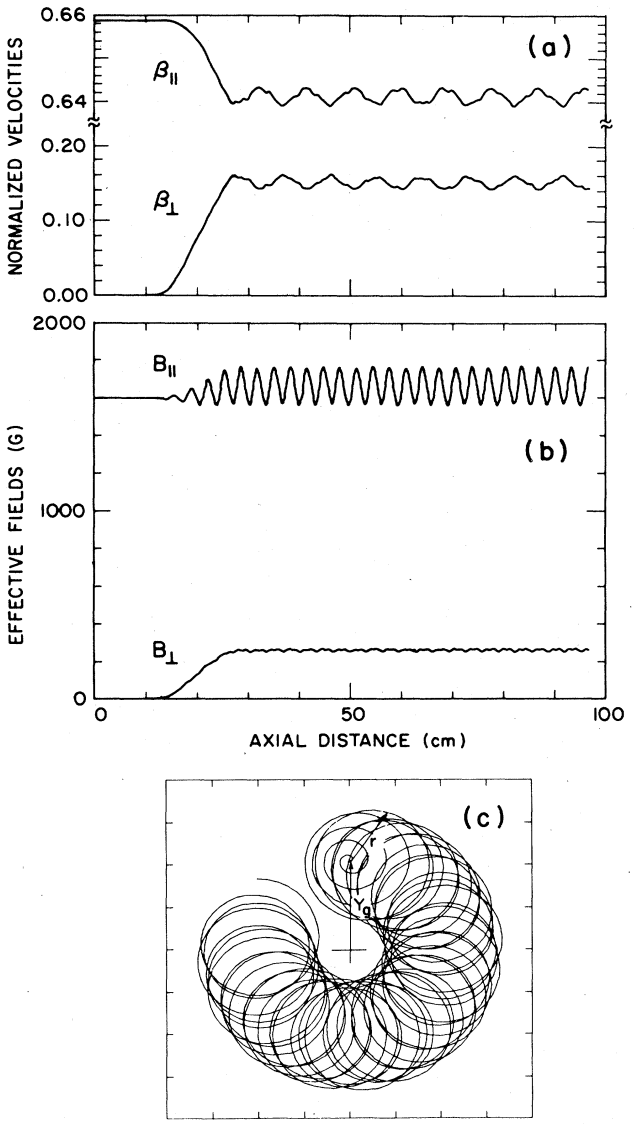


FIG. 1. Electron velocity and magnetic field variations as a function of distance $z$; $\gamma=1.33$, $k_w=1.904$, $B_w=250$ G, $B_a=1600$ G. The electron is started at the off-axis position $k_w y_g=0.4$. The six-period adiabatic wiggler introduction begins at $z=10$ cm. (a) Normalized axial velocity $\beta_{||}$ and perpendicular velocity $\beta_{\perp}$. (b) Axial magnetic field $B_{||}$ and perpendicular magnetic field $B_{\perp}$ at the instantaneous position of the electron. (c) Projections of the electron orbit onto the $x$-$y$ plane, illustrating azimuthal precession (Ref. 7).

$\beta_{\perp}=v_{\perp}/c$, and, in the constant-wiggler-amplitude region, the axial velocity $\beta_{||}$ is seen to oscillate around an average value $\langle\beta_{||}\rangle$. The average axial velocity $\langle\beta_{||}\rangle$ determines the FEL output frequency, and the average perpendicular velocity $\langle\beta_{\perp}\rangle$ determines the gain. Thus, precise comparisons between FEL theory and experiment require an accurate method of predicting $\langle\beta_{||}\rangle$ and $\langle\beta_{\perp}\rangle$ as a function of $y_g$, the radial distance from the axis of an electron's guiding center. Recently, Freund and Ganguly[5] have shown that (under the rather restrictive conditions discussed below) the expression for $\langle\beta_{\perp}\rangle$ for an off-axis electron is approximately given by

$$\langle\beta_{\perp}\rangle=\frac{\Omega_w\langle\beta_{||}\rangle I_0(k_w y_g)}{k_w\langle\beta_{||}\rangle c-\Omega_a}\ , \tag{6}$$

which when solved in conjunction with the energy-conservation equation [Eq. (2)], yields the values of $\langle\beta_{||}\rangle$ and $\langle\beta_{\perp}\rangle$.

The purpose of this paper is to derive a more general equation for $\langle\beta_{\perp}\rangle$. Although the derivation is of a semiempirical nature, we will show that it agrees well with single-particle computer simulations and with FEL experiments. Moreover, we shall demonstrate that our equation correctly approaches the results of the previous analyses; namely, when $y_g\rightarrow 0$, we recover the axis-centered results given by Eq. (5), and when $\lambda\rightarrow 0$, we recover Eq. (6). We note that the range of $y_g$ of practical interest is typically $k_w y_g<0.5$. In this range the quasihelical electron orbits are of sufficient quality to yield good FEL frequency and gain characteristics. When $k_w y_g>1$ the large betatron oscillations (see Fig. 1) cause serious deterioration of the FEL operation.

## ANALYTIC DERIVATIONS AND NUMERICAL SIMULATIONS

It is instructive to examine the origin of the correction terms in Eq. (5) [i.e., those terms not found in Eq. (3)]. As an electron moves away from the wiggler axis, it must respond to the axial component of the full wiggler field [Eq. (4)]. [On axis, at $r=0$, this component vanishes since $I_1(0)=0$.] Normally the axial component is oscillatory; however, for the special case of perfect axis-centered orbits, the axial component is constant because $\phi-k_w z=\text{const}$. Thus the electron is affected by a net axial field given by

$$B_{||}=B_a+2B_w I_1(\lambda)\ . \tag{7}$$

The off-axis increase in the perpendicular wiggler-field component is similarly constant, and the electron feels a net perpendicular field

$$B_{\perp}=2B_w I_1(\lambda)/\lambda\ . \tag{8}$$

Note that if we define $\Omega_{\perp,||}=eB_{\perp,||}/\gamma m_0 c$ and rewrite Eq. (5) as

$$\beta_{\perp}=\frac{\Omega_{\perp}\beta_{||}}{k_w\beta_{||}c-\Omega_{||}}\ , \tag{9}$$

then the axis-centered three-dimensional theory and the one-dimensional theory are functionally equivalent.

Because the denominator of Eq. (5) is small for parameters near resonance, the difference between the one-dimensional theory and the three-dimensional theory is largely due to the axial field correction. Since this correction is inherently a finite Larmor radius effect, it would not be found in a pure guiding-center theory such as that given by Eq. (6).

Numeric analysis of off-axis electron trajectories for a wide variety of system parameters shows that the average velocity $\langle\beta_{||}\rangle$ can be accurately predicted by Eq. (9) if the

fields $B_\perp$ and $B_\parallel$ are set equal to the *average* axial and perpendicular fields seen by the off-axis electron as it propagates along its trajectory. For example, an electron propagating with the parameters stated in the caption to Fig. 3(b), initially at radius $k_w r = 0.6$, has a numerically determined average axial velocity of $\langle \beta_\parallel \rangle = 0.905\,68$. The numerically determined average fields are $\langle B_\perp \rangle = 646.0$ G and $\langle B_\parallel \rangle = 129\,04$ G. If these fields are used in Eq. (9), the calculated average axial velocity is $\langle \beta_\parallel \rangle = 0.905\,54$, in good agreement with the numerically derived value given above. Thus analytic expressions for $\langle B_\perp \rangle$ and $\langle B_\parallel \rangle$ could be used to determine a semiempirical formula for non-axis-centered orbits.

Expressions for $\langle B_\perp \rangle$ and $\langle B_\parallel \rangle$ can be found if the electrons are assumed to travel without precession (see Fig. 2) in perfectly circular orbits around an off-axis guiding center, and are assumed to have the same phase relationship. That is, all the electrons at a given axial position travel in the same radial direction. This direction is taken to be the direction of an electron in an axis-centered orbit [Eq. (5)]. Without any loss of generality, the electron guiding centers can be assumed to be on the $\hat{\mathbf{e}}_y$ axis and, at the position $z=0$, the electron will be at the point on its orbit that is farthest away from the wiggler axis (Fig. 2). Then the exact expression for the wiggler field along the electron orbit is

$$\mathbf{B} = \hat{\mathbf{e}}_z B_a + 2B_w \left[ -\hat{\mathbf{e}}_r I_1'(k_w R)\sin(\varphi - k_w z + \alpha) - \hat{\mathbf{e}}_\phi \frac{I_1(k_w R)}{k_w R}\cos(\varphi - k_w z + \alpha) + \hat{\mathbf{e}}_z I_1(k_w R)\cos(\varphi - k_w z + \alpha) \right], \tag{10}$$

where $R^2 = r^2 + y_g^2 + 2 r y_g \cos\theta$, $\varphi = \phi - \pi/2 = \tan^{-1}[r\sin\theta/(y_g + r\cos\theta)]$, $y_g$ is the distance of the guiding center from the axis, $\theta$ is the angular position of the electron along its orbit, and $\alpha = 0$ or $\pi$ depending on whether $\Omega_a < k_w \langle \beta_\parallel \rangle c$ or $\Omega_a > k_w \langle \beta_\parallel \rangle c$. The average transverse field is

$$\langle B_\perp \rangle = 2B_w \left\langle \left[ [I_1'(k_w R)]^2 \sin^2(\varphi - k_w z) + \left[ \frac{I_1(k_w R)}{k_w R} \right]^2 \cos^2(\varphi - k_w z) \right]^{1/2} \right\rangle \tag{11}$$

and the average axial field is

$$\langle B_\parallel \rangle = B_a + 2B_w \langle I_1(k_w R)\cos(\varphi - k_w z) \rangle \cos\alpha , \tag{12}$$

where the averages $\langle\ \rangle$ on the right-hand sides of the above equations are to be taken over the orbit angle $\theta$, and are carried out by expanding in $y_g$ and $r$. The calculation becomes extremely involved if higher-order terms are included. Consequently the symbolic manipulation program MACSYMA (Ref. 6) is used to perform the calculations. However, we note that as a result of the rapid betatron oscillations, the perfect-circular-orbit assumption is no longer a good approximation when the axial magnetic field $B_a$ is very small or zero.

The procedure employed is to expand the formulas for $\langle B_\perp \rangle$, $\langle B_\parallel \rangle$, $R$, and $\varphi$ in Taylor series to fourth-order terms in $y_g$ and $r$. Expansion of $\varphi$ also requires the assumption that either $y_g \ll r$ or $y_g \gg r$. The Taylor series for $\langle B_\perp \rangle$ and $\langle B_\parallel \rangle$ is equivalent to a power series in sines and cosines, and can easily be averaged by integrating over the orbit angle $\theta$. The resultant series is then identified as the sum of modified Bessel functions plus small residual terms. The average perpendicular field is found to be

$$\langle B_\perp \rangle \approx 2B_w I_0(k_w y_g)[I_1(\lambda)/\lambda](1 + \epsilon_{\lessgtr}) , \tag{13}$$

where

$$\epsilon_< \approx \frac{k_w^4 y_g^2}{6144}(k_w^4 r^4 y_g^2 - 24 k_w^2 r^2 y_g^2 + 24 y_g^2 - 8 k_w^2 r^4 + 96 r^2) \tag{14}$$

for $y_g \ll r$, and

$$\epsilon_> \approx \frac{k_w^4 y_g^2}{256}(k_w^2 r^2 y_g^2 - y_g^2 - 4r^2) \tag{15}$$

for $y_g \gg r$. For $k_w y_g < 1$, $\epsilon$ is typically less than 0.001, and can be ignored. The distinction between $y_g \ll r$ and $y_g \gg r$ is a mathematical artifact; there is no physical discontinuity separating these two parameter regimes. Thus it is evident that to within an error of $\epsilon_{\lessgtr}$,

$$\langle B_\perp \rangle \approx 2B_w I_0(k_w y_g) I_1(\lambda)/\lambda \tag{16}$$

for all parameter regimes where $r$ and $y_g$ are sufficiently small. The average axial field is similarly found to be

$$\langle B_\parallel \rangle \approx B_a + 2B_w I_0(k_w y_g) I_1(\lambda) \tag{17}$$

which, to fourth order, is exact for both $y_g \ll r$ and $y_g \gg r$. Substituting these two terms into the velocity relation Eq. (9) yields the sought-after expression for $\langle \beta_\perp \rangle$:

$$\langle \beta_\perp \rangle = \frac{2\Omega_w \langle \beta_\parallel \rangle I_0(k_w y_g) I_1(\lambda)/\lambda}{k_w \langle \beta_\parallel \rangle c - \Omega_a - 2\Omega_w I_0(k_w y_g) I_1(\lambda)} . \tag{18}$$

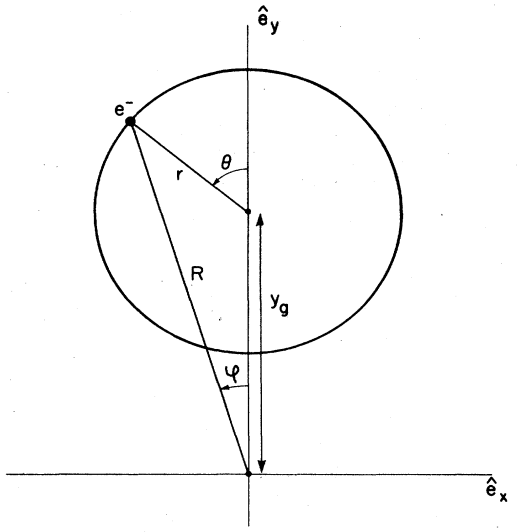


FIG. 2. Coordinate system used in the derivation of Eq. (10). Precession seen in Fig. 1(c) is neglected here.

In the limit $y_g \to 0$, this expression reduces to the axis-centered theory represented by Eq. (5), and in the limit $\lambda \to 0$, the expression is identical to the guiding-center theory represented by Eq. (6).

The parameters $\langle \beta_{\parallel} \rangle$ and $\langle \beta_{\perp} \rangle$ are obtained by a simultaneous solution of Eqs. (2) and (18). The value of $y_g$ employed in solving Eq. (18) is the initial electron radius in the $B_w = 0$ region outside the wiggler. In Fig. 3 the predicted values of $\langle \beta_{\parallel} \rangle$ (solid dots) are compared with the values of $\langle \beta_{\parallel} \rangle$ obtained by numeric simulation for a wide range of parameters (curved lines). For $k_w y_g < 0.6$, the worst case error is $(\langle \beta_{\parallel} \rangle_{\text{sim}} - \langle \beta_{\parallel} \rangle_{\text{theor}}) / \langle \beta_{\parallel} \rangle_{\text{sim}} < 0.0003$. In Fig. 3(b) we also show the predictions of the previously derived, pure guiding-center theory [Eqs. (2) and (6)]. While this theory exhibits the correct qualitative behavior, it is significantly less precise than the results obtained from Eq. (18).

The complete three-dimensional field along the electron orbit of Eq. (10) oscillates around the average field values given by Eqs. (16) and (17) and the oscillation may be substantial, particularly for the axial field (see Fig. 2). A more detailed description of the electron orbits allowing for azimuthal and radial drifts can be found by considering the total magnetic field to be a superposition of the average field denoted as $\langle \mathbf{B}_0 \rangle$ and a small perturbation $\mathbf{B}_1$. If the velocity is decomposed into a small perturbation $\mathbf{v}_1$ around the average velocity $\langle \mathbf{v}_0 \rangle$, then, to first order,

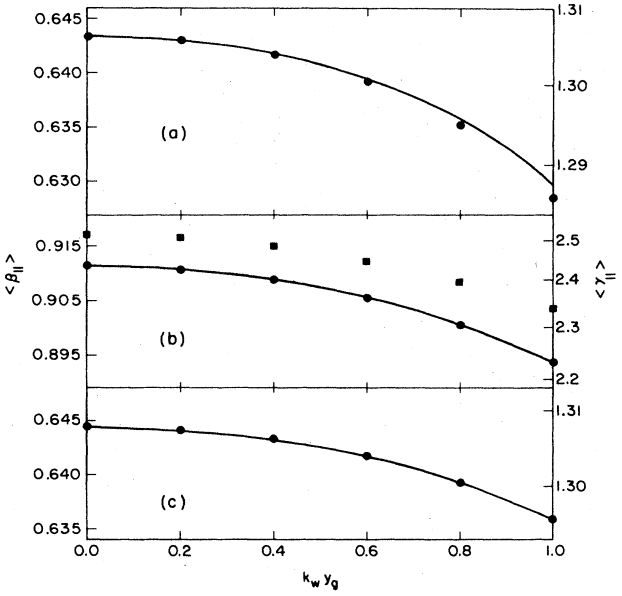


FIG. 3. Average axial velocity $\langle \beta_{\parallel} \rangle$ as a function of the normalized distance of the electron guiding centers from the wiggler axis $k_w y_g$. Curves are the value of $\langle \beta_{\parallel} \rangle$ found numerically, and the dots give the theoretical prediction of Eqs. (2) and (18). (a) $\langle \beta_{\parallel} \rangle$ for $\gamma = 1.33$, $B_w = 250$ G, $k_w = 1.904$, $B_a = 1600$ G. (b) $\langle \beta_{\parallel} \rangle$ for $\gamma = 3.4$, $B_w = 583.3$ G, $k_w = 2.904$, $B_a = 13\,120$ G. (c) $\langle \beta_{\parallel} \rangle$ for $\gamma = 1.33$, $B_w = 250$ G, $k_w = 1.904$, $B_a = 4000$ G. (a) is for trajectories well below resonance ($k_w \langle \beta_{\parallel} \rangle c > \Omega_a$), (b) is for trajectories very near resonance, and (c) is for trajectories well above resonance. (b) also shows (squares) the predictions of the pure guiding-center theory of Eqs. (2) and (6).

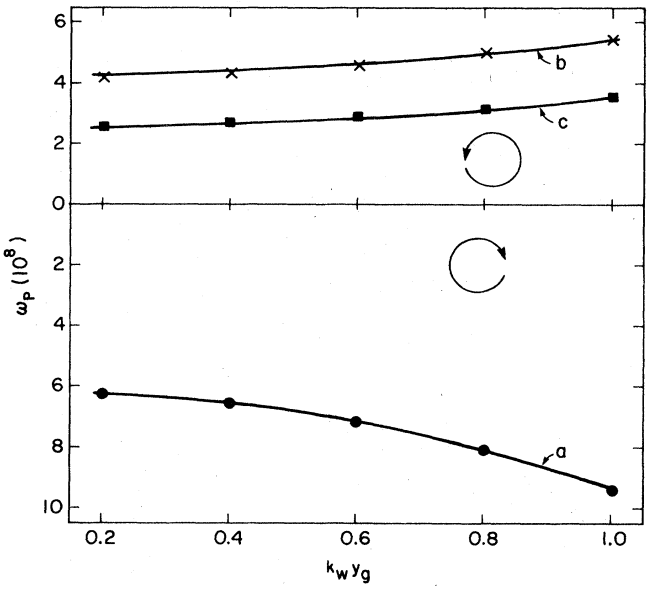


FIG. 4. Precession frequency $\omega_P$, of the electron guiding centers as a function of the normalized distance of the electron guiding centers from the wiggler axis $k_w y_g$. Computer simulations are shown by the lines, and the predictions of Eq. (20) are given by the dots. Cases *a*, *b*, and *c* correspond to the configurations of Figs. 3(a), 3(b), and 3(c), respectively. Arrow indicates the direction of the precession, which changes sign as $k_w \beta_{\parallel} c \gtrless \Omega_a$.

$$\frac{d\mathbf{v}_1}{dt} \approx \frac{e}{\gamma mc} (\mathbf{v}_1 \times \langle \mathbf{B}_0 \rangle + \langle \mathbf{v}_0 \rangle \times \mathbf{B}_1) \,. \tag{19}$$

This equation was solved to first order in $r$ in the limit $r \ll y_g$, and it was found that $\mathbf{v}_1$ is equal to a sum of oscillatory terms at the fundamental and harmonics of $k_w z$, and an azimuthal drift which causes the guiding center to precess around the wiggler axis[7] [Fig. 1(c)]. To this order, there is no radial drift. However, the numeric simulations show that there is a small outward drift for electrons that are situated very far away from the axis ($k_w y_g > 1$).

In Fig. 4 the precession frequency predicted by Eq. (19),

$$\omega_P = \frac{c}{y_g} \frac{B_w \langle \beta_{\perp} \rangle I_1(k_w y_g)}{B_a - 2B_w I_0(k_w y_g) I_1(\lambda)} \quad (B_a \neq 0) \,, \tag{20}$$

is compared with the numerically determined precession frequency. The excellent agreement between the theory and the simulations shown in Figs. 3 and 4, and the lack of any large radial drifts, confirm the empirical assumptions underlying the derivations.

## EXPERIMENTS

The validity of Eq. (18) has been confirmed experimentally by measuring the spectral properties of a free-electron laser[8,9] as a function of the position of the FEL's electron beam relative to the FEL wiggler axis. An electron beam produced by a Marx-generator-driven thermionic electron gun is constrained to flow along the axis of a solenoidal magnet. The superimposed bifilar helical

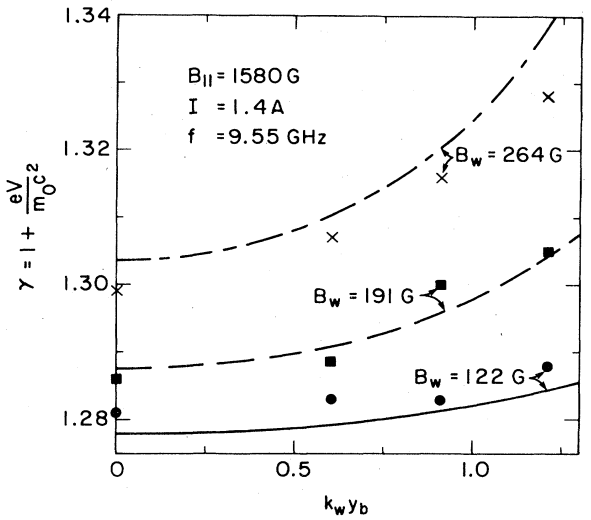


FIG. 5. Experimental results showing the energy required to radiate a fixed frequency $\omega/2\pi=9.55$ GHz as a function of the normalized distance of the electron beam from the wiggler axis $y_b$. Data are given for three values of the wiggler field. Experimental points are shown by the crosses, squares, and dots, and the predictions of Eqs. (2), (18), and (21) are given by the lines.

wiggler magnet induces amplification in a codirectional microwave signal of known amplitude and known frequency $\omega$. Amplification occurs only at the appropriate beam energies corresponding to the radiation frequency[10]

$$\omega=\beta_{||}ck_{w,\text{eff}}\gamma_{||}^2 \times\{1+\beta_{||}[1-(\omega_c/k_{w,\text{eff}}\gamma_{||}\beta_{||}c)^2]^{1/2}\} . \quad (21)$$

Here the effective wiggler wave number is $k_{w,\text{eff}}=k_w-p_1\omega_p\Phi^{1/2}/\gamma^{1/2}\gamma_{||}\beta_{||}c$; $\omega_p=(Ne^2/m_0\epsilon_0)^{1/2}$ is the nonrelativistic plasma frequency; $\omega_c=(\omega_{c0}^2+p_2^2\omega_p^2/\gamma)^{1/2}$ is the effective waveguide cutoff frequency adjusted for the presence of the electron beam; $\omega_{c0}$ is the empty-waveguide cutoff frequency; $p_1$ and $p_2$ are frequency-dependent numerical factors, less than unity, that are related to the finite transverse geometry of the system; and $\Phi$ is a correction to the space-charge dispersion equation due to the combined presence of the axial and wiggler magnetic fields, and is defined as

$$\Phi=1-\{\Omega_{||}\gamma_{||}^2\beta_w^2/[(1+\beta_w^2)\Omega_{||}-k_w\beta_{||}c]\} , \quad (22)$$

where $\beta_w=\beta_\perp/\beta_{||}$ is the normalized transverse velocity acquired by the electrons from the wiggler magnetic field.[10]

The wiggler is mounted so that it can be moved freely in the direction transverse to the axial solenoid field. Note that the solenoid axis and the wiggler axis remain collinear. Since the position of the center of the electron beam is defined by a 0.254-cm-radius aperture centered on the solenoid axis, the wiggler position can be adjusted so that the electron beam propagates through the wiggler at any desired distance $y_b$ from the wiggler axis. In this way the beam electrons are allowed to sample different axial and perpendicular wiggler-field components and amplitudes as prescribed by Eq. (4). In Fig. 5 we plot the experimentally determined beam energy required to radiate the fixed frequency $\omega/2\pi=9.55$ GHz, as a function of the distance between the beam center $y_b$ and the wiggler axis. The dashed and solid lines show the theoretically predicted beam energy as determined by solving Eqs. (2), (18), and (21). We have taken $y_g$ in Eq. (18) to be equal to $y_b$. The experimental data agree well with the predictions of the general three-dimensional theory. However, the good agreement should be considered with caution since the beam diameter is large and only somewhat smaller than the beam displacement $y_b$.

## DISCUSSION

In the past, there has been some discussion in the FEL community concerning the merits of the various orbit approximations [Eqs. (3), (5), and (6)] when an electron beam of finite thickness propagates in realistic helical wiggler and guide magnetic fields. Users of the one-dimensional theory [Eq. (3)] or the guiding-center theory [Eq. (6)] have questioned, with some justification, the use of the axis-centered theory [Eq. (5)] for beams of considerable thickness, typically $k_w r_b \approx 0.5$, in which the beam radius and the electron undulations are of comparable size. On the other hand, comparisons with experiments described here and in earlier studies[9] have consistently shown better agreement with the axis-centered theory [Eq. (5)]. In this paper we find, by comparisons with numeric simulations, that the axis-centered approximation is always a better representation of the electron dynamics than the one-dimensional theory [Eq. (3)] and for small values of $y_g$ it is also better than the guiding-center theory. We also obtain a precise and general result, given by Eq. (18), that can be used for a thick electron beam. This formula accurately predicts the results of numeric simulations, and it agrees well with experimental observations. Consequently, the orbit expression Eq. (18) developed here can be used with assurance over the full range of beam radii of practical interest ($k_w r_b < 1$).

## ACKNOWLEDGMENTS

This work was supported in part by the National Science Foundation, in part by the Hertz Foundation, and in part by the U. S. Air Force Office of Scientific Research.

[1]L. Friedland, Phys. Fluids 23, 2376 (1980).
[2]J. Fajans, G. Bekefi, and B. Lax, Proceedings of the IEEE Conference on Plasma Science, Ottawa, 1982 (IEEE, New York, 1982) p. 18.
[3]P. Diament, Phys. Rev. A 23, 2537 (1981).
[4]H. P. Freund, S. Johnston, and P. Sprangle, IEEE J. Quantum Electron. QE-19, 322 (1983).
[5]H. P. Freund and A. K. Ganguly, IEEE J. Quantum Electron. QE21, 1073 (1985).
[6]R. Pavelle, M. Rothstein, and J. Fitch, Scientific American

245, 130 (1981).
[7]J. A. Pasour, F. Mako, and C. W. Roberson, J. Appl. Phys. 53, 7174 (1982).
[8]J. Fajans, G. Bekefi, Y. Z. Yin, and B. Lax, Phys. Rev. Lett. 53, 246 (1984).
[9]J. Fajans, G. Bekefi, Y. Z. Yin, and B. Lax, Phys. Fluids 26, 1995 (1985).
[10]H. P. Freund and P. Sprangle, Phys. Rev. A 28, 1835 (1983).